Multi-Task Network-Based Confinement Mode Identification, Instability Detection and Disruption Prediction in EAST Plasma

Yunhu.Jia[1,2] , Wenhui.Hu[1,*], Qingquan.Yang[1], Xin.Lin[1], Bihao.Guo[1], Adi.Liu[2], JiLei.Hou[1]
Zhengping.Luo[1], Yuehang.Wang[1], Yao.Huang[1], RuiRui.Zhang[1], Qiping.Yuan[1], Bingjia.Xiao[1,2,3]

[1] *Institute of Plasma Physics, Hefei Institutes of Physical Science, Chinese Academy of Sciences*
[2] *University of Science and Technology of China*
[3] *Institute of Energy, Hefei Comprehensive National Science Center*

*Email: huwh@ipp.ac.cn

Outline

Introduction

Methods

Results and discussion

Future work

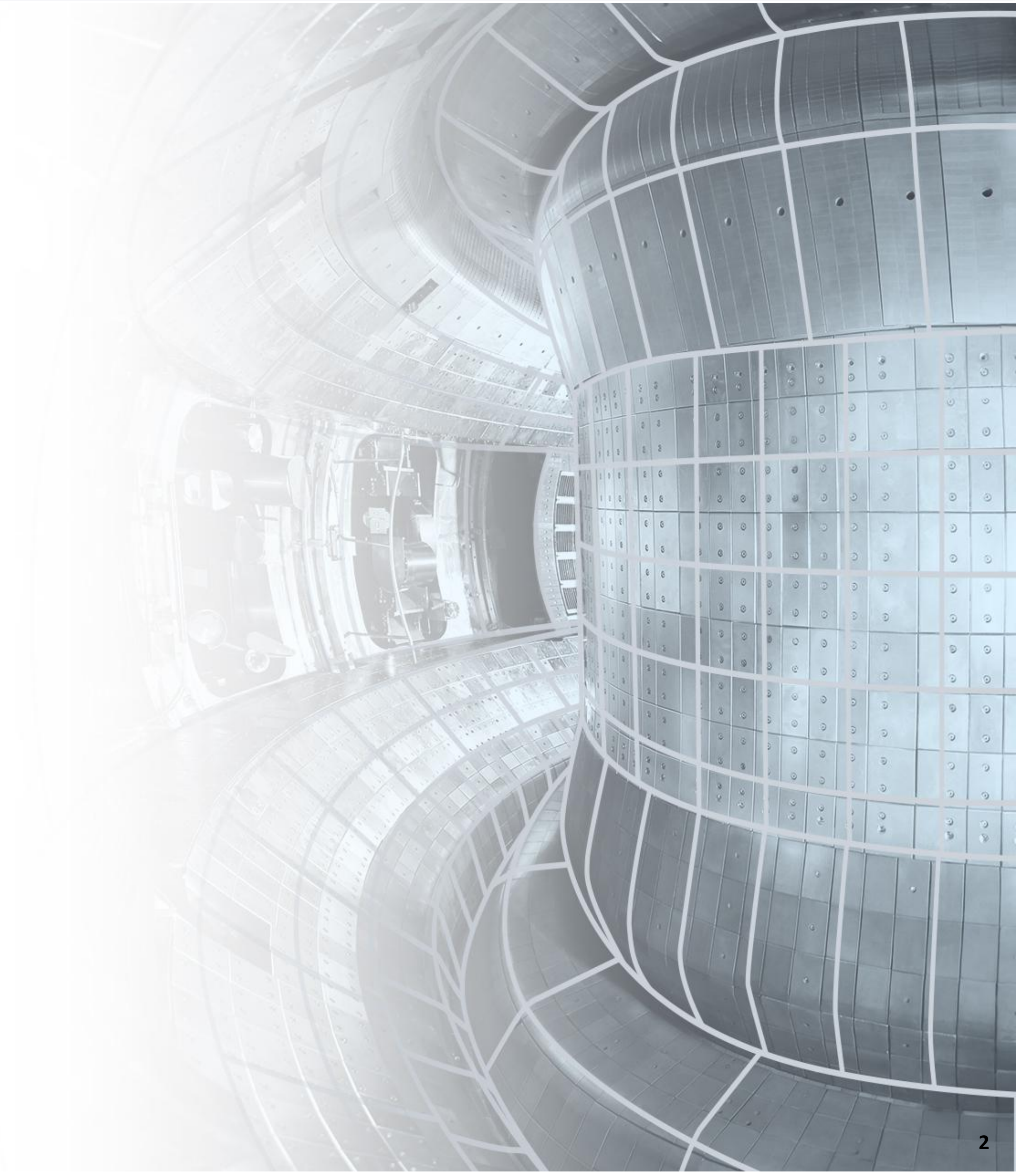

Background

- Plasma disruption can seriously damage tokamak. It's crucial to reliably assess plasma disruptivity to avoid or mitigate its impact.
- Before a disruption, plasma usually goes through a complex chain of precursor events, such as an increase in plasma instabilities and unexpected transitions in confinement modes. So, these precursor events also need to be monitored to ensure timely action.[2-4].

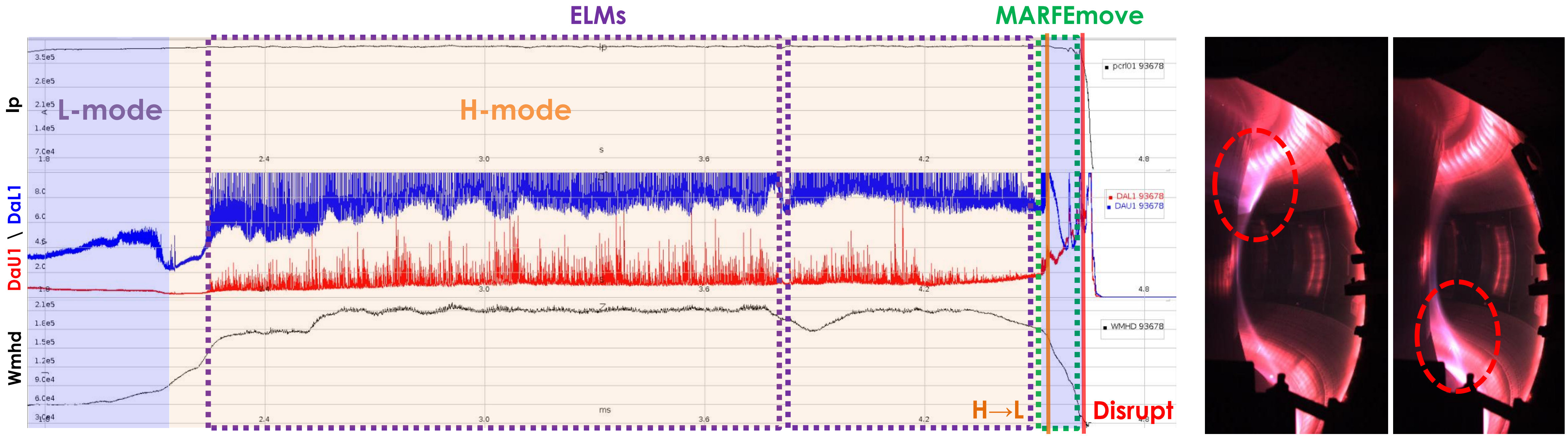

Figure 1. (Left) Event Chain of a Disruption Ending Shot (EAST #93678); (Right) MARFE Movement Observed in Camera

[1] de Vries, et al.(2016). Requirements for Triggering the ITER Disruption Mitigation System. Fusion Science and Technology, 69(2), 471–484.

[2] Diamond, Patrick H., et al. “How the Birth and Death of Shear Layers Determine Confinement Evolution: From the L → H Transition to the Density Limit.” Philosophical Transactions of the Royal Society A: Mathematical, Physical and Engineering Sciences, vol. 381, no. 2242, Feb. 2023, p. 20210227.

[3] Seo, Jaemin, et al. “Avoiding Fusion Plasma Tearing Instability with Deep Reinforcement Learning.” Nature, vol. 626, no. 8000, Feb. 2024, pp. 746–51.

[4] Orozco, David, et al. “Neural Network-Based Confinement Mode Prediction for Real-Time Disruption Avoidance.” IEEE TRANSACTIONS ON PLASMA SCIENCE, vol.50, no.11,Nov 2022,pp. 4157–64,

Related Research

ASIPP

- Assessing disruptivity and monitoring its precursors with first-principles methods is difficult[5]
- Recent works highlight the potential of machine learning methods in these tasks. (Table 1)
- Notably, some studies combine these tasks into a unified model(multi-task model), improving the performance and interpretability of disruption prediction[7].
- However, **EAST lacks such multi-task models**,and creating a high-performance, easily transferable one is still a major challenge.

Table 1: Current State of Related Research

Tasks	Methods and Research Content	Device	Performance	References
Disruption Prediction	A review on disruption prediction with artificial intelligence techniques	-	-	J. Vega, et al. Nature Phys. 18, 741-750(2022)
	CNN+Attention+MMD: Model trained on EAST carbon wall database,then transferred to metal wall database.	EAST	AUC: 0.97/0.93	[11] Guo B H, et al. 2023 Nucl.Fusion 63 094001
Instability detection	Random Forest: Prediction of MARFE-movement	EAST	ACC 85%–90%	Hu W H, et al. Chin. Phys. B 32, 075211 (2023)
	TCNN+LSTM: Identification of MHD	EAST	ACC: 98.38%	Lingyi Kong et al 2024 PlasmaPhys.Control.Fusion 66 015016
Confinement Mode identification	MLP: identification of H/I/L mode	EAST	ACC: 96.03%	[6] K.N. Yang,et al. Nucl. Fusion 64 (2024) 016035 (11pp)
	CNN: Real-time identification of H/L mode	DIII-D	ACC: 98%	David Orozco, et al. IEEE TPS, VOL.50, NO.11, 2022
	Attention+LSTM: identification of H/L mode	TCV	κ-statistic: 0.94	F.Matos,et al. Nucl. Fusion 61 (2021) 046019 (11pp)
Multiple tasks integrated	**Multi-task learning: detect various instability events and simultaneously predict disruptions.**	**DIII-D**	**AUC: 0.94**	**[7] Zhu J X, et al. Nucl. Fusion 63 (2023) 046009 (14pp)**

[5] De Vries P.C., Pautasso G., Humphreys D., Lehnen M., Maruyama S., Snipes J.A., Vergara A. and Zabeo L. 2016 Fusion Sci. Technol. 69 471–84

Our work

- We developed a multi-task model that can predict disruptions, detect macro-instabilities (ELMs and MARFE Movement), and identify confinement modes (H/I/L mode or just ohmic heating) all at once.
- In EAST carbon wall database, Our multi-task model achieved best performance in disruption prediction and ELMs detection, and outperformed single-task models in other tasks.
- As shown in Fig. 2, our model takes the current time and a 100ms data window before it as input. The output is the result of various tasks at the current time. All signals come from the Plasma Control System (PCS) with a 1 kHz sampling rate, making the model suitable for real-time applications in the future.

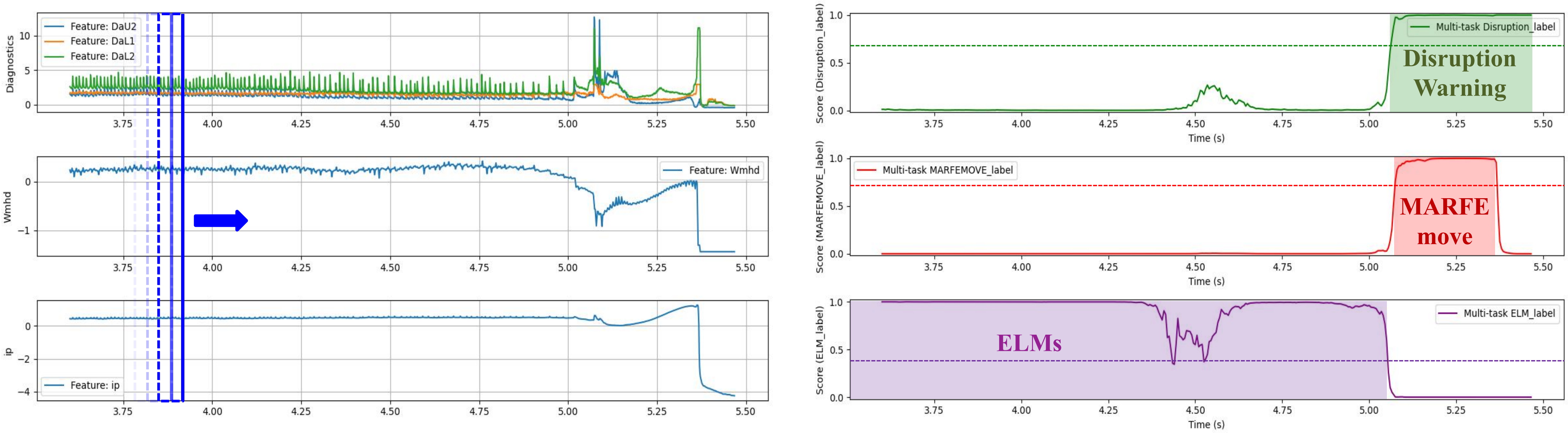

Figure 2. Examples of Partial Input and Output of Our Multi-Task Model

Outline

Introduction

Methods

Results and discussion

Future work

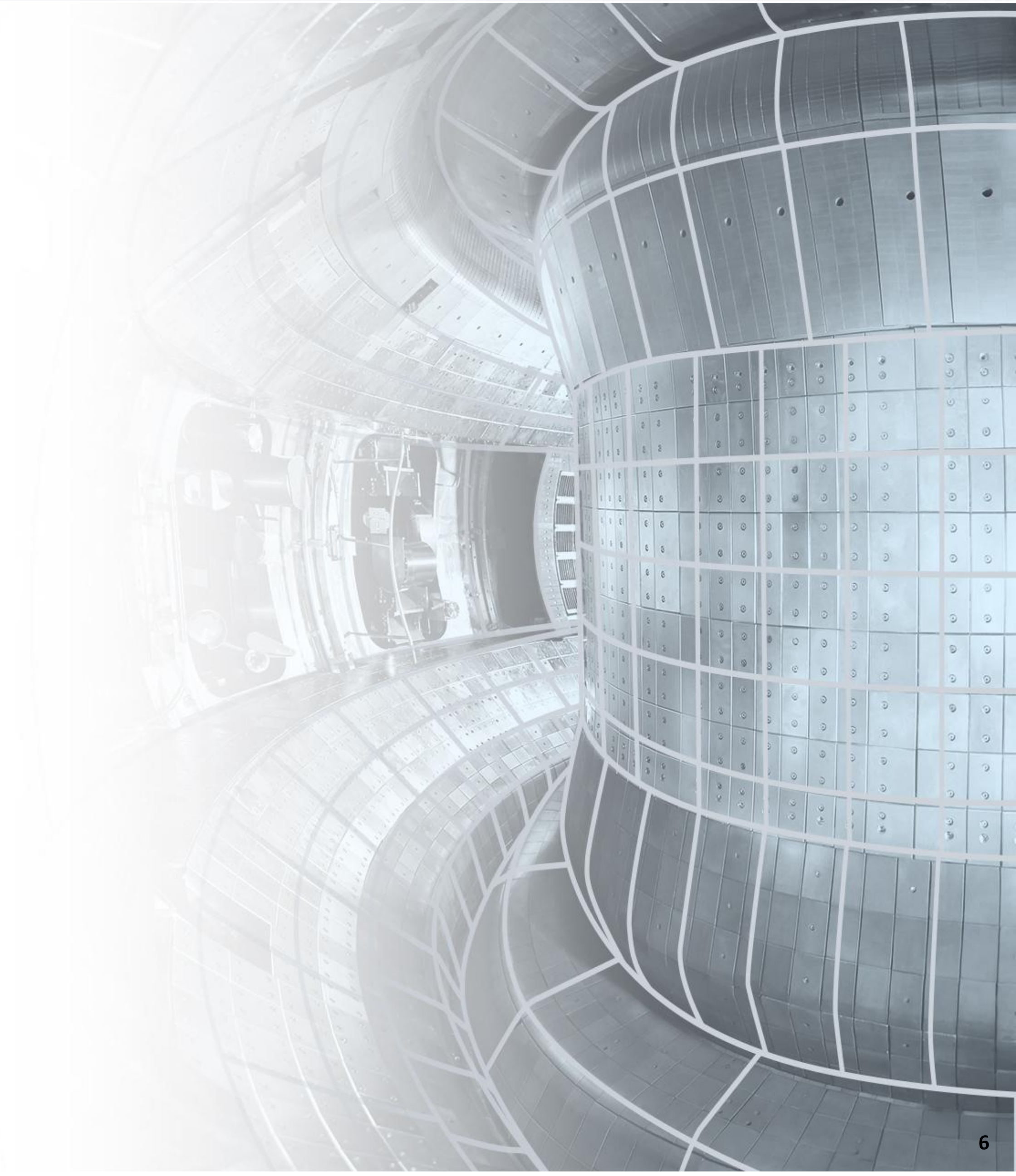

Data source

- Our multi-task dataset is from 9756 EAST discharges (2015-2020). Data from 2020 onwards are from the metal wall environment, while earlier data are from the carbon wall environment.
- The dataset includes extensive labels for disruptions, instabilities, and confinement modes, all provided by reliable experts who have extensively studied these phenomena on EAST[6,8,9,10].Due to limited expert resources, instability and confinement mode labels cover only part of the shots.
- The dataset is divided by shot numbers(Table 2). For comparison with previous disruption predictions, the disruptive/undisruptive shot numbers in each dataset match those in Guo's research[11] exactly.

Table 2: Dataset division (The unit of Pos/Neg time is seconds)

Annotation	Training Set	Validation Set	Carbon Wall Test Set	Metal Wall Test Set
Disruption	Shots Number:6516 disruptive shots:1993	Shots Number:1399 disruptive shots:431	Shots Number:1234 disruptive shots:437	Shots Number:297 disruptive shots:80
ELM	Shots Number:130 Pos Time:401.94,Neg Time:517.81	Shots Number:29 Pos Time:63.08,Neg Time:136.69	Shots Number:31 Pos Time:70.01,Neg Time:154.4	Shots Number:133 Pos Time:531.5,Neg Time:682.86
MARFEmove	Shots Number:21 Pos Time:7.61,Neg Time:56.8,	Shots Number:5 Pos Time:4.48,Neg Time:10.9	Shots Number:6 Pos Time:3.68,Neg Time:13.86	Shots Number:49 Pos Time:24.62,Neg Time:370.8
H_Mode	Shots Number:84 Pos Time:422.37,Neg Time:0.0,	Shots Number:15 Pos Time:71.69,Neg Time:0.0	Shots Number:16 Pos Time:74.07,Neg Time:0.0	Shots Number:101 Pos Time:532.2,Neg Time:0.0
I_Mode	Shots Number:53 Pos Time:80.6,Neg Time:0.0,	Shots Number:17 Pos Time:24.44,Neg Time:0.0	Shots Number:21 Pos Time:31.94,Neg Time:0.0	Shots Number:19 Pos Time:39.74,Neg Time:0.0
L_Mode	Shots Number:46 Pos Time:80.4,Neg Time:0.0,	Shots Number:10 Pos Time:26.82,Neg Time:0.0	Shots Number:19 Pos Time:38.48,Neg Time:0.0	Shots Number:10 Pos Time:101.1,Neg Time:0.45
OHM_Mode	Shots Number:26 Pos Time:131.06,Neg Time:0.0,	Shots Number:10 Pos Time:43.57,Neg Time:0.0	Shots Number:10 Pos Time:52.77,Neg Time:0.0	Shots Number:21 Pos Time:107.72,Neg Time:0.0

Input Signal

- We chose plasma signals for this study based on literature[4-10], PCS availability, EAST researchers suggestions, and minimizing signal numbers.
- Utilizing Short-Time Fourier Transform (STFT) on Da signals to extract time-frequency information for feature enhancement, we obtained 22 input signals (Table 3).

Table 3: Signal Selection

Symbol	Signal description	Symbol	Signal description
p_RAD	Radiated power	rad_input_frac	$\frac{Radiated\ power}{Input\ power}$
DaL1	Deuterium Balmer-a line emission spectrum (lower first channel)	DaU2	Deuterium Balmer-a line emission spectrum (upper second channel)
ne	Electron density	Z_cur_lmsz	Linearly estimated vertical displacement
ip	Plasma current	pxuv32	Bolometric radiation measurement
Wmhd	Plasma stored energy	p_LH	Lower hybrid heating power
v_loop	Loop voltage	kappa	Elongation ratio
ip_error_normalized	$\frac{Plasma\ current - Programed\ plasma}{current\ Programed\ plasma}$	Greenwald_fraction	$\frac{Electron\ density}{Greenwald\ density}$
q95	Safety factor at the 95% flux surface	ne_error	density – current programed plasma density
STFT_DaU2_50-100Hz	STFT of DaU2 in the 50-100 Hz range	STFT_DaL1_50-100Hz	STFT of DaU2 in the 50-100 Hz range
STFT_DaU2_100-150Hz	STFT of DaU2 in the 100-150 Hz range	STFT_DaL1_100-150Hz	STFT of DaL1 in the 100-150 Hz range
STFT_DaU2_150-200Hz	STFT of DaU2 in the 150-200 Hz range	STFT_DaL1_150-200Hz	STFT of DaL1 in the 150-200 Hz range

[8] Kim, S.K., Shousha, R., Yang, S.M. et al. Highest fusion performance without harmful edge energy bursts in tokamak. Nat Commun 15, 3990 (2024).
[9] Hu, Wenhui, et al. "Prediction of Multifaceted Asymmetric Radiation from the Edge Movement in Density-Limit Disruptive Plasmas on Experimental Advanced Superconducting Tokamak Using Random Forest." Chinese Physics B, vol. 32, no. 7, July 2023, p. 075211. Institute of Physics,
[10] W.H. Hu, et al. "Real-Time Prediction of High-Density EAST Disruptions Using Random Forest." Nuclear Fusion, vol. 61, no. 6, June 2021, p. 066034.

Our Model Structure

- Our model has a feature extractor and several task classifiers. The feature extractor is a multi-scale convolutional network[6], and the task classifiers are linear fully connected neural networks.
- To enhance performance, we constructed cascade relationships between task classifiers, creating a second model structure.
- Model input: using the current time and the preceding 100ms window of signals from Table 3 as input, forming a 100*22 matrix.
- All hyperparameters are obtained using a genetic algorithm on the validation set.

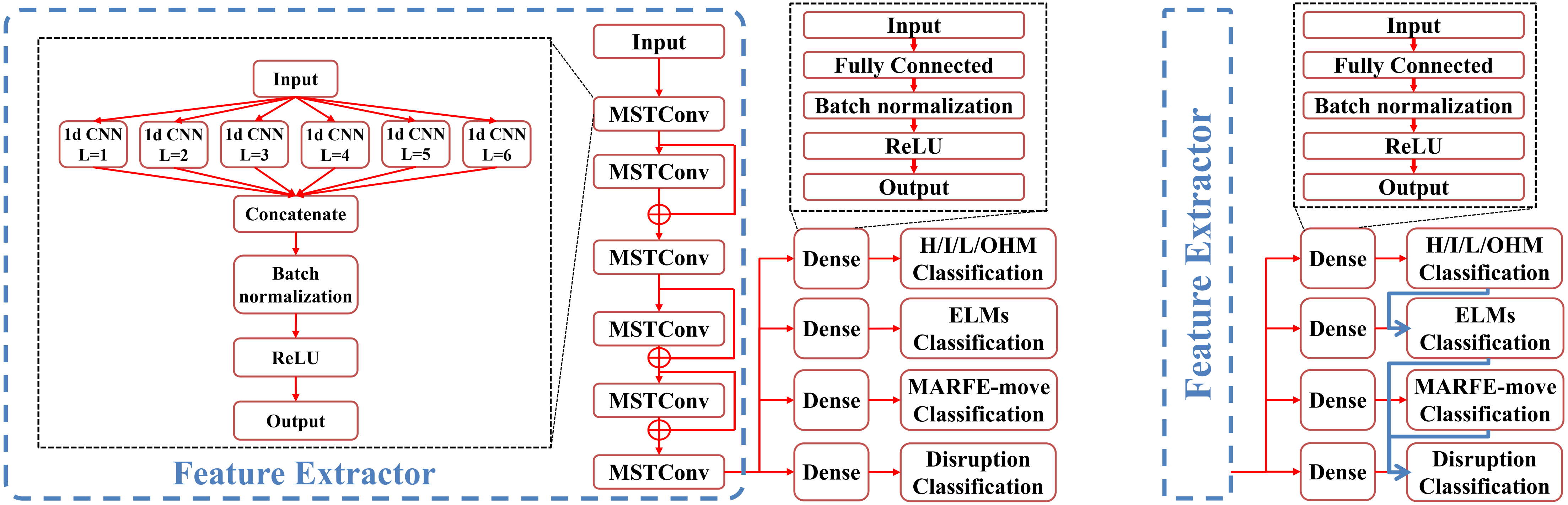

Figure 3. (Left) Parallel configuration of task classifiers; (Right) Cascade configuration of task classifiers.

Outline

Introduction

Methods

Results and discussion

Future work

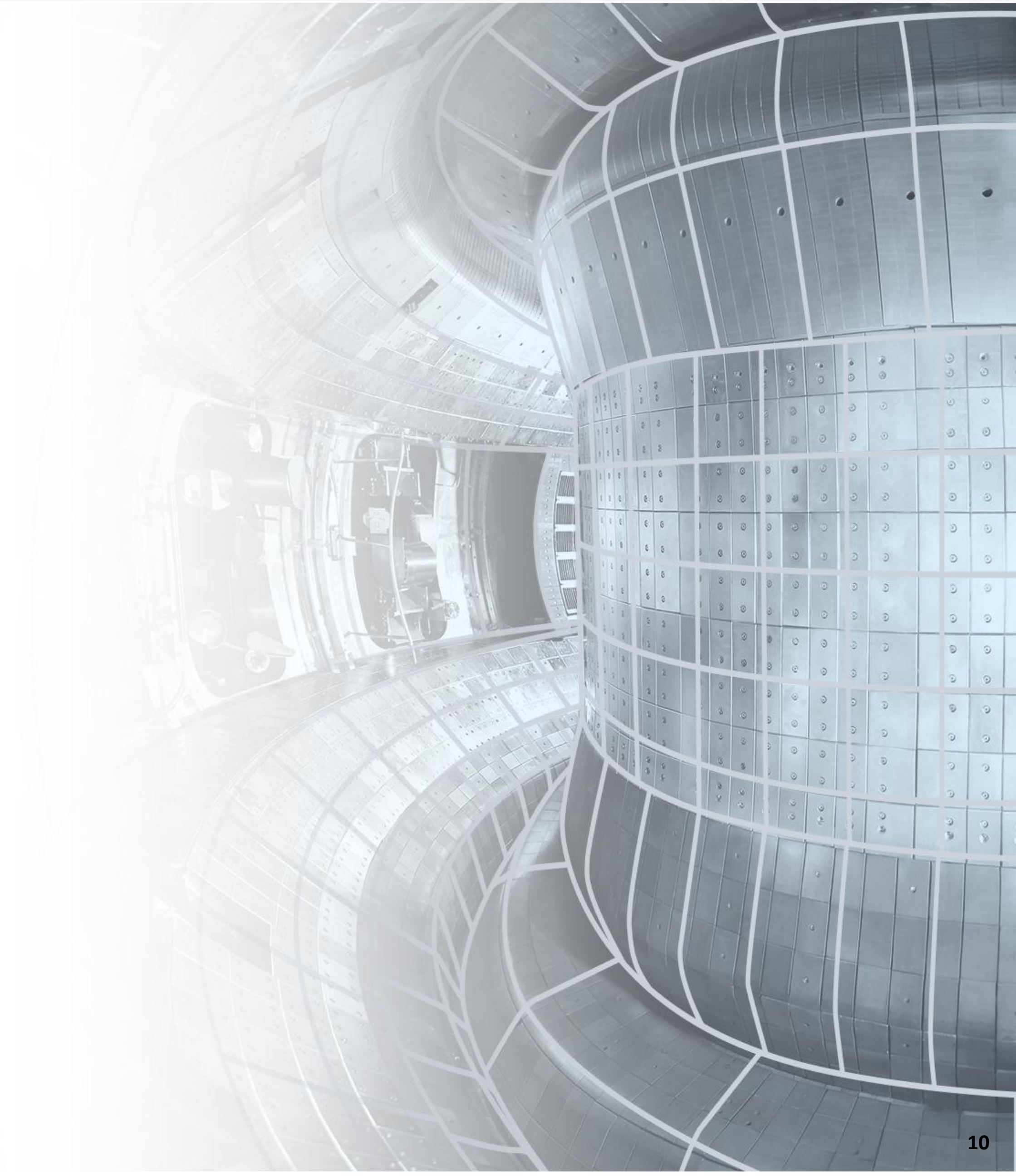

Best disruption prediction: multi-task cascade model

- For disruption prediction, the multi-task model is more accurate and gives earlier warnings than the single-task model.
- Also, the multi-task cascade model achieves the best performance(AUC 0.98 and Mean warning time 1.146s) on the EAST carbon wall database (previous record[10] was AUC 0.97 and Mean time 0.755s).

This ROC curve shows the True Positive Rate vs. False Positive Rate for different thresholds. The red line indicates random guessing (AUC = 0.5). Higher AUC means better performance.

The x-axis shows the lead time before disruption (warning time), and the y-axis shows the fraction of disruptions detected by that time.

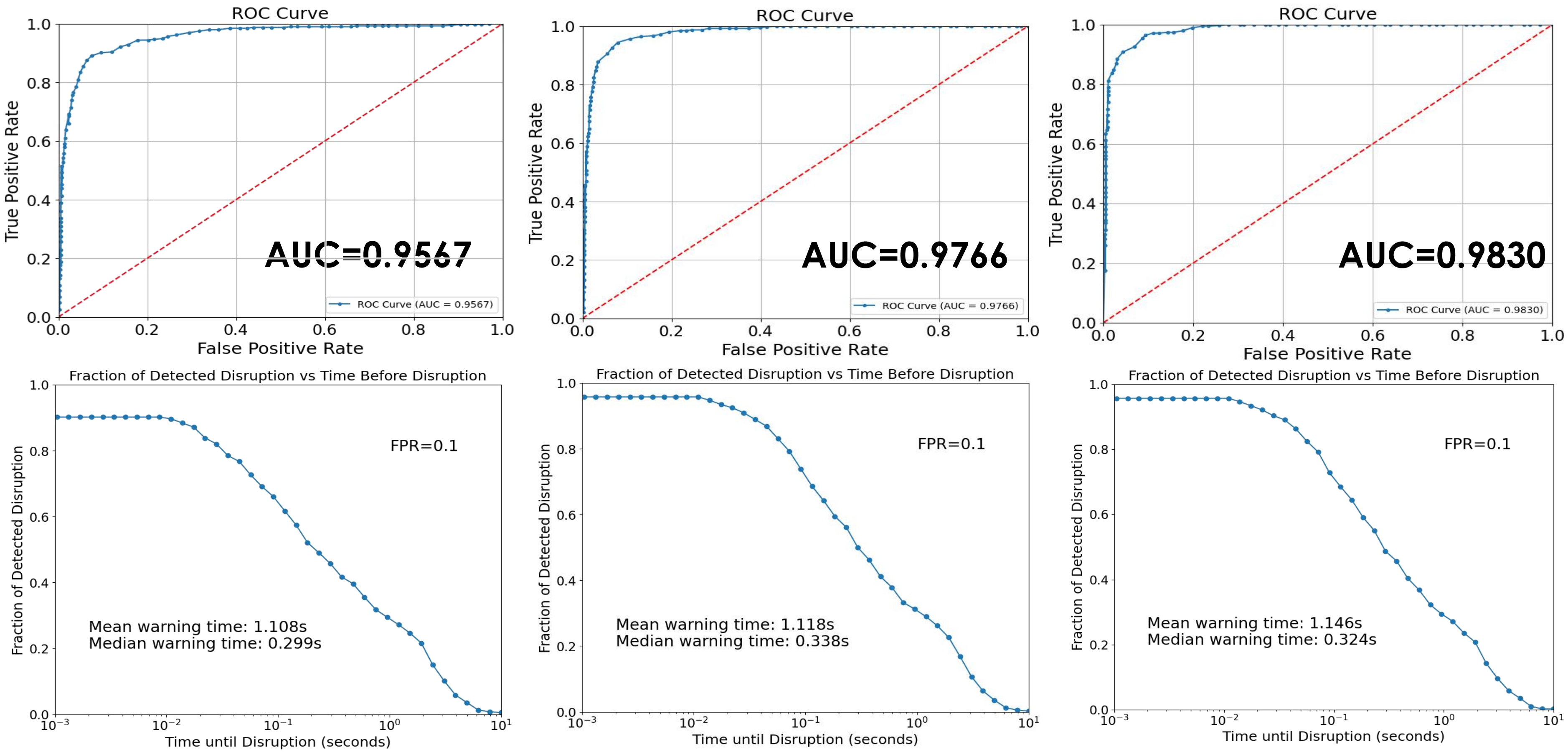

Figure 4: (Left) Single-task model; (Middle) Multi-task parallel model; (Right) Multi-task cascade model.

Best instability detection: multi-task cascade model

- The multi-task cascade network outperforms the multi-task parallel network in instability detection, which is better than single-task models.
- The ELM detection AUC of multi-task cascade network is 0.991, the best performance so far on EAST carbon wall database.

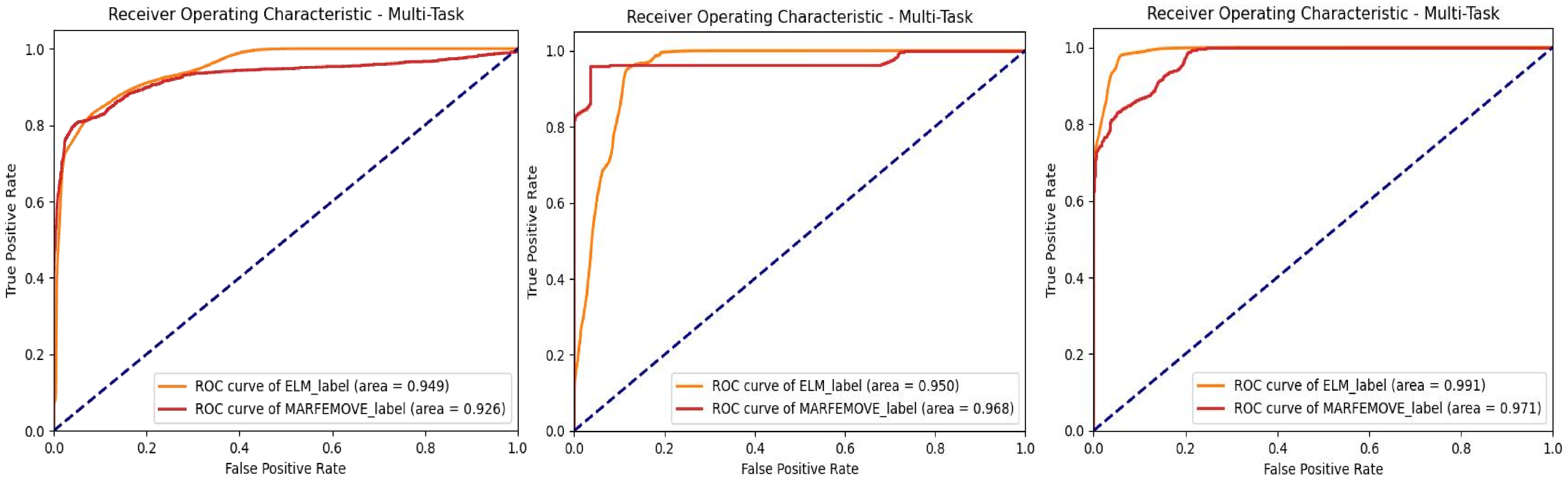

Figure 5: (Left) Single-task model; (Middle) Multi-task parallel model; (Right) Multi-task cascade model.

Correlation between instability detection and disruption prediction

- Through multi-task joint learning, it was observed that instability detection tasks impact disruption prediction(Fig.6), enhancing both interpretability and performance of the predictions.
- The detection score of ELMs is negatively correlated with disruptivity, while the detection score of MARFE movement is positively correlated with disruptivity. This implies the presence of ELMs decrease disruptivity, while MARFE movement increases it,matching experimental experience.
- Specifically, although ELMs may lead to more severe instabilities, they do not directly cause disruptions. Stable ELM behavior indicates orderly energy release at the plasma edge, representing lower disruptivity.

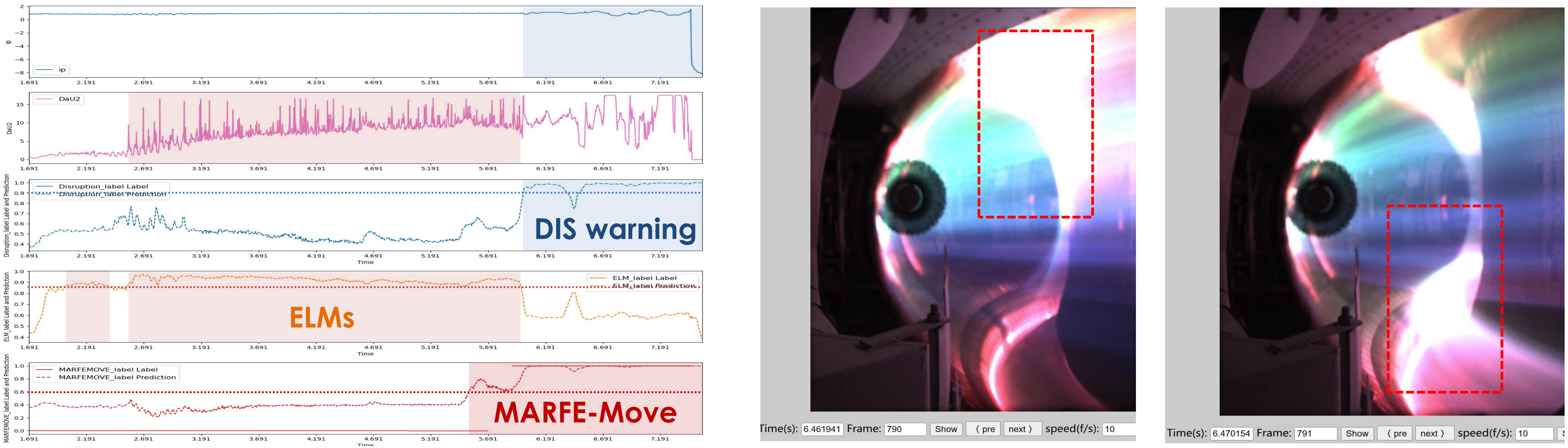

Figure 6. Instability detection and disruption prediction impact each other (EAST Test Shot: 70611)

Best Confinement Mode Identification: multi-task parallel model

ASIPP

- For confinement mode identification, the model outputs the class with the highest score directly. Therefore, model performance can be directly measured by the ACC from the confusion matrix.
- The best model is the multi-task parallel model, achieving an ACC 91.48%, which is below the performance reported in the literature[6]. However, our model doesn't need high-frequency signals to detect WCM, making the model suitable for real-time applications in the future.

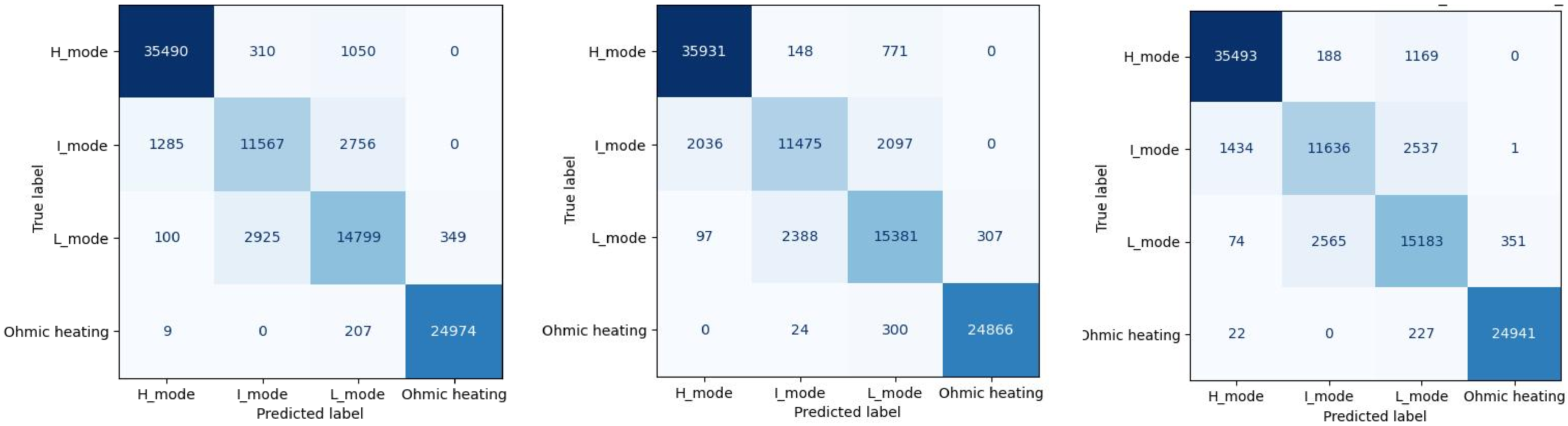

ACC 90.61% **ACC 91.48%** **ACC 91.06%**

Figure 7: (Left) Single-task model; (Middle) Multi-task parallel model; (Right) Multi-task cascade model.

Confinement Mode Transition Identification

- The model can identify H-mode, L-mode, I-mode, or just ohmic heating. It can also indirectly identify the transitions between different confinement modes.

- However, the accuracy of transition identification (Specific time of transition) needs improvement.

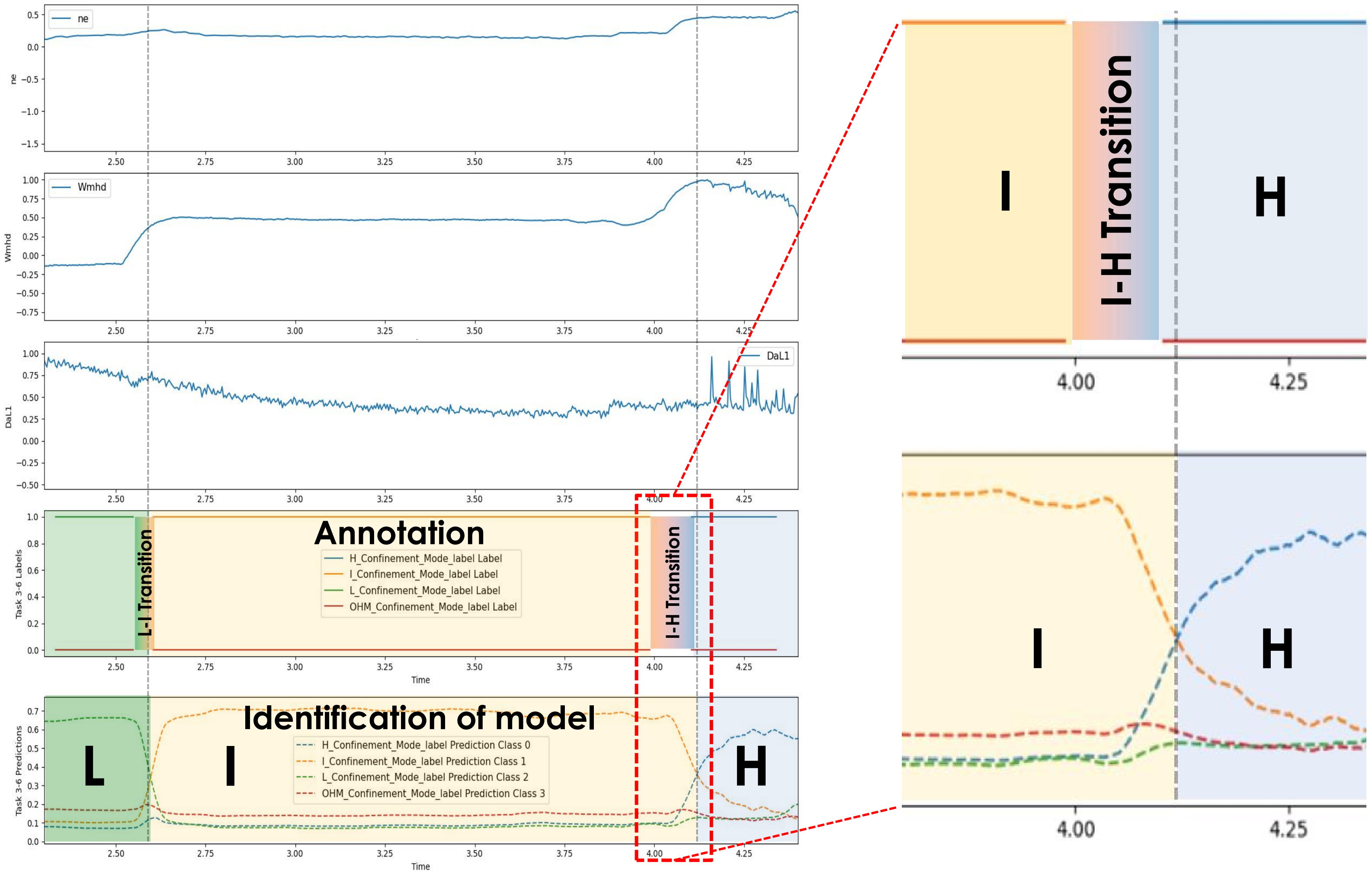

Figure 8. Confinement mode identification (EAST Test Shot: 77572)

Outline

Introduction

Methods

Results and discussion

Future work

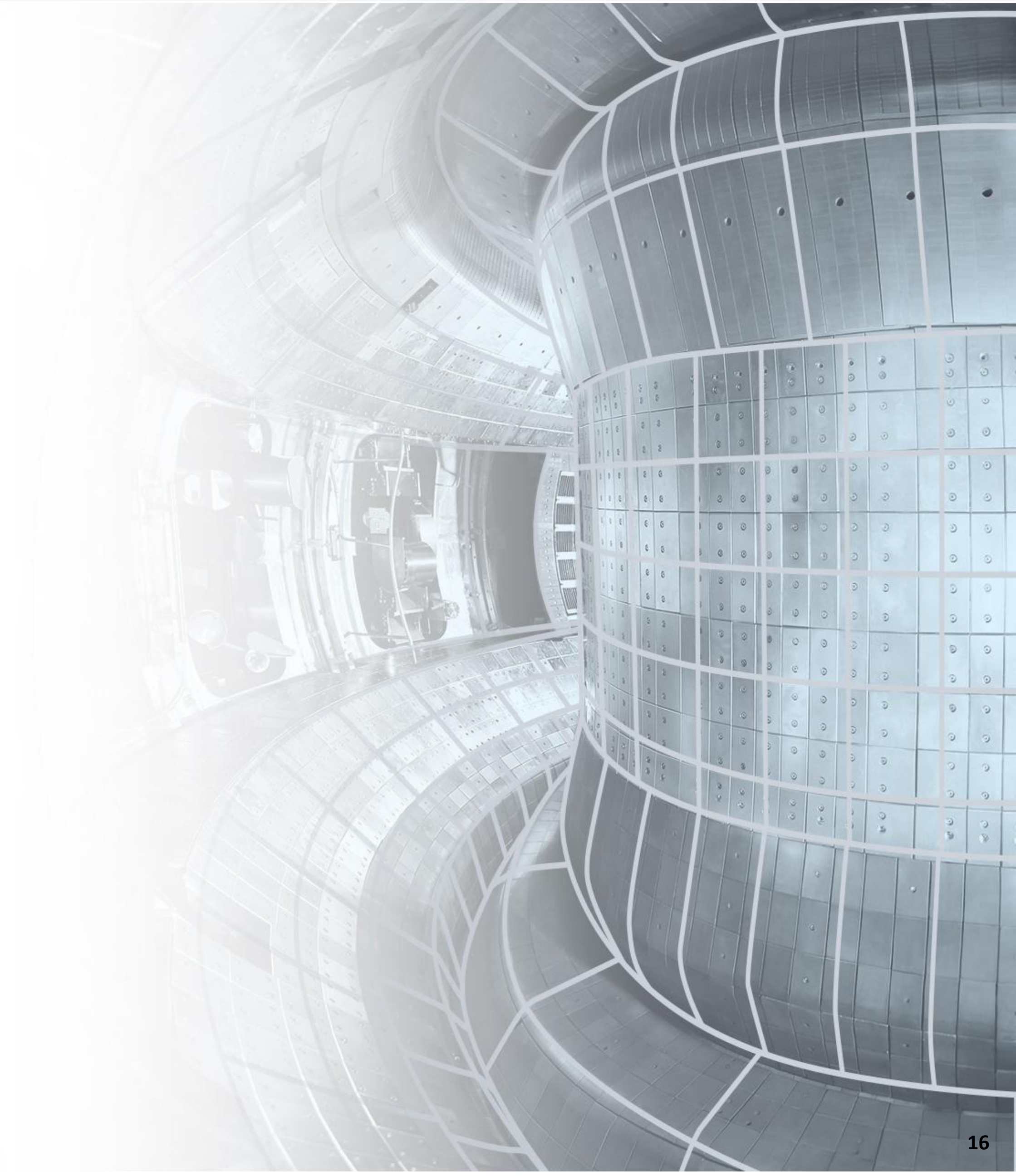

Enhancing Transition and Cross-Wall Performance

- To enhance the performance in identifying the specific time of transition, a specialized transition identification task is added based on the confinement mode recognition.
- To address the issue of performance degradation across walls[11], a domain adversarial task is added.

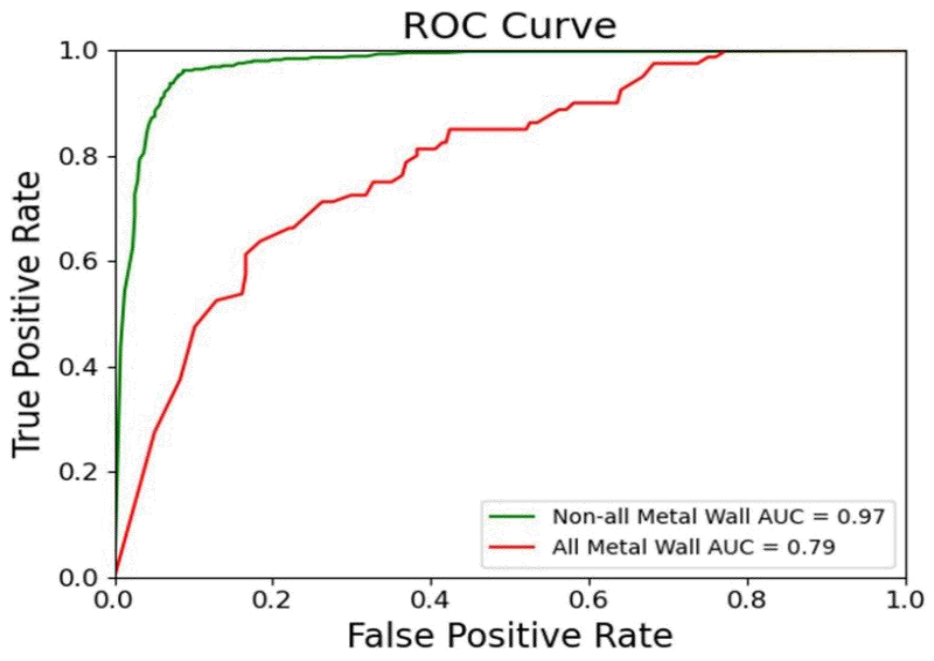

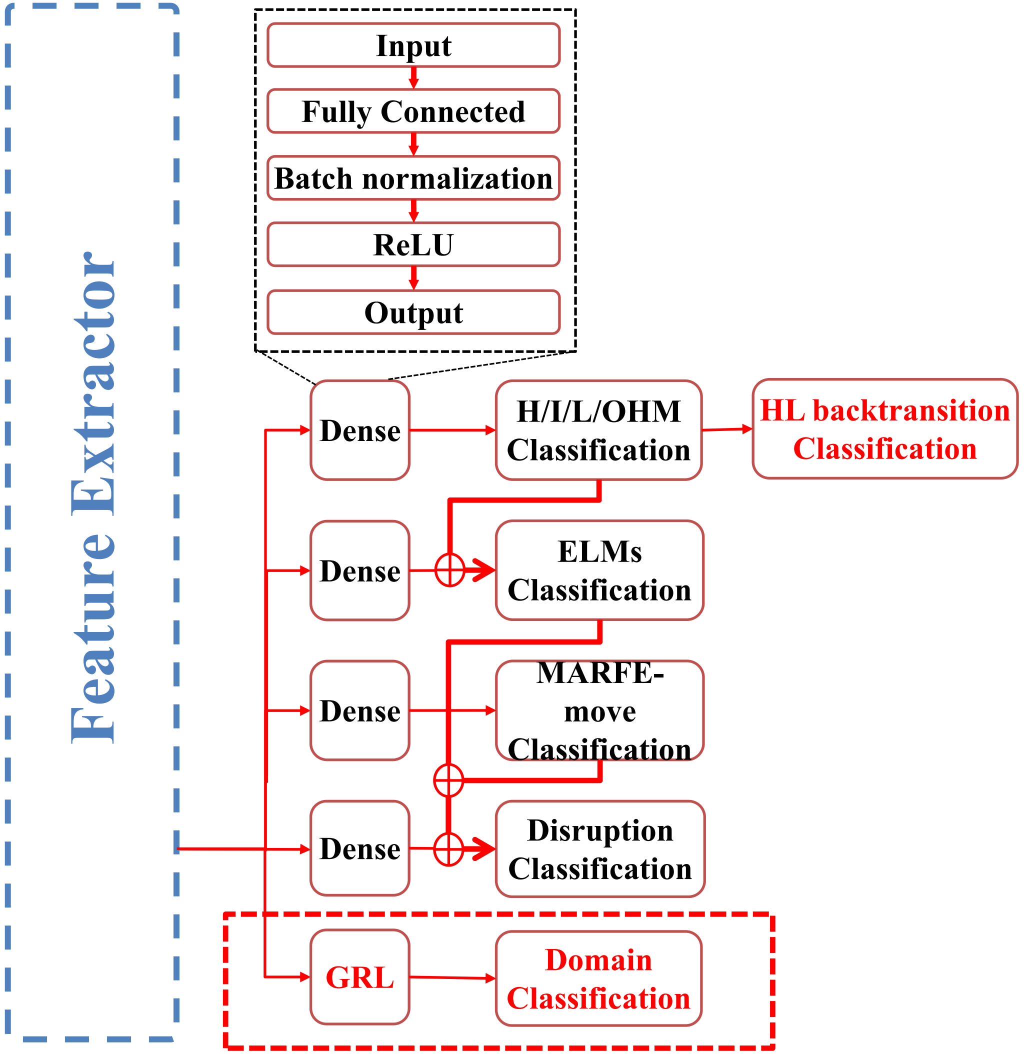

Figure 9. performance declines when working across walls[11]

Figure 10. Future model structure

[11] Guo, B. H., et al. Nuclear Fusion, vol. 63, no. 9, July 2023, p. 094001. Institute of Physics,

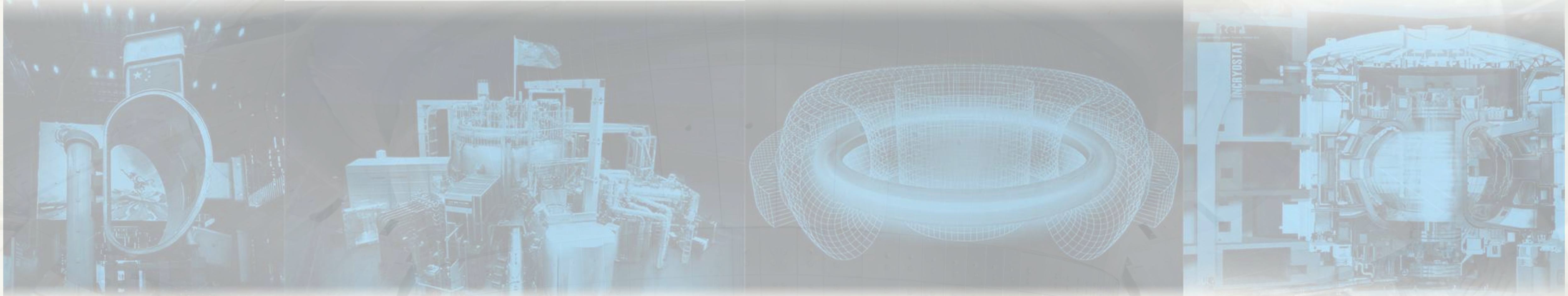

Thank you !